

GT-2005-68971

**DESIGN AND ANALYSIS OF A HIGH STAGE LOADING FIVE-STAGE LP TURBINE RIG
EMPLOYING IMPROVED TRANSITION MODELING**

Jochen Gier and Norbert Hübner

MTU Aero Engines GmbH
Munich, Germany

ABSTRACT

Modern aircraft engine designs have to realize high performance while managing important weight and cost issues. For high bypass ratio engines this results in high demands for the low pressure turbine component. The combination of a low speed parameter due to large fan diameters with reduced number of turbine stages due to weight and cost considerations leads to high stage loading requirements. Realizing high turbine efficiencies at low Reynolds Number operation at high altitudes for these high stage loadings is a key for state-of-the-art turbofan engines.

For the aerodynamic design, high stage loading factors directly translate into increased airfoil flow turning. These increased turning levels have to be realized in combination with elevated airfoil load in order to keep low airfoil counts. This is particularly challenging in combination and requires minimization of negative effects on the airfoil losses and secondary losses.

In this paper the development of a five-stage turbine with high stage loading is discussed with focus on the aerodynamic design. A specially designed cascade test has been part of the turbine design, which showed the need for improvement of the transition modeling within the CFD code used for design and analysis. The derived modeling enhancement is then employed for the analysis of the five-stage rig, which was tested at the altitude test facility at Stuttgart University. The modeling achieved significant improvements in the quality of the numerical results. The analysis includes sensitivities to Reynolds number and a detailed view of the suction side flow.

NOMENCLATURE

AF	[-]	amplification factor
BF	[-]	factor
C	[-]	constants

b_{ax}	[m]	axial chord
c_{ax}	[m/s]	axial velocity component
f	[1/s]	frequency
f_t	[-]	intermittency factor
h	[m]	airfoil height
Δh	[kg/kJ]	specific (total) enthalpy difference
H_{12}	[-]	boundary layer form parameter
L	[m]	true chord
N	[-]	number
n_{rel}	[1/s]	relative rotational speed
n_{crit}	[-]	turbulence parameter
p	[Pa]	pressure
p/c	[-]	pitch-to-chord ratio
Re	[-]	Reynolds number = $u_{exit} \cdot l / \nu$
Tu	[-]	turbulence degree
u	[m/s]	velocity
U	[m/s]	turning velocity
α, β, γ	[-]	coefficients
η	[-]	efficiency
ν	[m ² /s]	kinematic viscosity
ω	[1/s]	specific turbulence dissipation
$\zeta = \text{zeta}_v$	[-]	loss coefficient = $(p_{tim} - p_{tout}) / (p_{tout} - p_{out})$
Θ	[m]	momentum thickness

Subscripts

is	isentropic
red	reduced
t	total
0	inlet
∞	farfield

INTRODUCTION

The introduction of high by-pass ratio civil aero engines results in rigid constraints on the low pressure turbine component. These concepts lead to high power output requirements combined with reduced rotational speeds. On the other hand the low pressure turbine makes up a significant portion of the total engine weight and its efficiency has a large impact on total engine fuel burn.

Lower rotational speeds in combination with a weight driven reduction of the number of stages strongly impact the aerodynamics of the low pressure turbine as the relevant dimensionless parameter $\Delta h/U^2$ is forced to higher values. According to aerodynamic experience, which is documented for example in the well-known Smith chart [1], this translates into increased losses and thus reduced efficiency.

Aerodynamically, to achieve the same specific work output Δh with reduced rotational speed either leads to an equivalent increase in turbine diameter (to achieve unchanged turning velocities), which would add considerable weight, or results in a higher stage work coefficient $\Delta h/U^2$. According to the Euler turbine equation, for the same work output lower turning velocities have to be compensated by an increased difference of the circumferential velocities. This leads to higher flow deflection or higher though flow velocities. Both options result in higher Mach number levels in the turbine.

According to experience, e.g., Traupel [2] and Denton [3] this directly corresponds to higher airfoil losses. In addition, larger flow turning inside the airfoil rows in case of increased deflection as well as lower airfoil aspect ratios for squeezed high through flow annuli correspond to increased secondary flow losses, Gregory-Smith et al. [4], which add to the efficiency reduction.

Currently a typical stage loading factor for civil by-pass engines is in the area of $\Delta h/U^2 \approx 2$, although lower values would still offer efficiency benefits. There are a few reports in the open literature which deal with higher stage loading investigations.

In the 70's very high stage loading turbines were developed and tested within the E³ program in the United States. The turbines had stage loading factors $\Delta h/U^2$ of 4.5 in 4 1/2 - stage turbines, Whitney et al. [5]. It was demonstrated that this level of stage loading is achievable, but the realized efficiencies would not be sufficient for today's civil aero engines.

Moustapha et al. [6], Schaub et al. [7] and Vlasic et al. [8] have published a series of papers over some period of time addressing high stage loading turbine investigations. These were focused on high-pressure turbines with loading factors of up to 2.5. They investigated various aspects of these turbines from aerodynamic performance to tip leakage effects and cooling relevance.

Kawachi et al. [9] investigated a single stage high-pressure turbine with a stage loading factor of 2.1, which is not untypical for low pressure turbines. The same applies to the work of Haller and Anderson [10].

More recently, Vásquez et al. [11,12] reported on investigations into high stage loading low pressure turbines. They describe extensive investigations into concepts for high stage loading. They especially focus the on the choice for an optimal flow path concept comparing high (HTF) and low through flow (LTF) designs. These design variants are compared in terms of impact of airfoil design,

performance potential, acoustics and weight. Based on this they also developed a modified efficiency prediction for high stage loading turbines.

In the current paper the aerodynamic design of a low pressure turbine with a stage loading factor of 2.6 is described. This level is not the highest possible, however a high level of efficiency had to be maintained. The turbine has five stages and has been designed as a cold flow rig. It was tested in the altitude test facility at Stuttgart University with extensive instrumentation. To support the design of this turbine, preliminary design studies included a new linear cascade airfoil investigation with unsteady wake interaction.

Based on these investigations, the need for an improved transition model became obvious. The extension for the effects of wake interaction has been developed to support the rig airfoil design. A description is included in the paper.

DESIGN OF CASCADE AIRFOIL

Going to increased stage loads automatically leads to higher levels of deflection inside the airfoil rows, unless the c_{ax}/U is increased significantly. In order to gain additional basic information about the behaviour of LP turbine airfoils with elevated levels of turning and hence mitigate the associated risk for aerodynamic performance, a cascade test was set up. Experience with LP turbine airfoils for cascade testing was mainly available for turnings up to 100°, e.g., the widely used T106 airfoil.

These cascades were installed in plane constant height channels, which for typical velocity triangles lead to acceleration ratios of about 2. For an increased turning, this would have resulted in even higher flow acceleration, which is not representative of high stage loading turbines, where acceleration is reduced compared to more conventional designs.

Therefore, the new cascade was designed inside a diverging channel in order to decouple the increased turning from the acceleration. Based on this cascade, the sensitivity of losses with respect to the more adverse aerodynamic boundary conditions could be studied. Furthermore, the data could be used to check the quality of the boundary layer flow description in the analysis tools, especially in the transition modeling of the Navier-Stokes code. A short summary of the integral airfoil characteristics is given in table 1.

	T160	T106A
turning [°]	107.0	100.0
vel. ratio	1.6	2.05
p / c	0.8	0.8
Zweifel	0.96	0.88
inflow angle [°]	133.0	127.7
exit angle [°]	25.7	26.5
h / b_ax (@inlet)	2.85	3.5

Table 1: Comparison of selected parameters of T160 and T106A

A three-dimensional view of the T160 cascade can be seen in figure 1. The channel passage is becoming divergent upstream of the airfoil to assure the designed streamtube thickness at midspan. The airfoil was designed using 2D-Euler combined with a boundary layer and a Navier-Stokes analysis code. The design features a controlled balance between the accelerating and diffusing parts of the suction side. The airfoil loading was chosen reasonably high with a Zweifel

number close to 1. Comparing it to the T106A, a typical feature of high stage loading velocity triangles can be seen as the swirl component of the inflow angle is changed much more compared to the swirl component of the exit angle.



Figure 1: Cascade T160 in divergent channel

The experiments were performed in the high-speed wind tunnel of the University of Armed Forces in Munich. Several Re-numbers (70k to 400k) and Mach-numbers (Ma2: 0.2 and 0.6) were investigated. In order to at least approximately assess the influence of incoming wakes in a real turbine the cascade was additionally tested with a moving bar wake generator, Stadtmüller [13]. Running the airfoil inside the divergent channel in combination with the wake generator proved quite challenging, because a wake generator also turns the flow by a couple of degrees. This leads to a changing incidence to the airfoil and has to be compensated in order to have comparable flow conditions.

IMPROVEMENT OF TRANSITION MODELING

As expected, the loss development as a function of the Reynolds number (Reynolds lapse rate) changed quite considerably by introducing the unsteady wakes. This effect has been reported several times e.g., Mayle [14], Hodson [15]. It can be seen in figure 2 by looking at the experimental data. The Re-lapse rate shows a reduced sensitivity for the case with the moving bars. This effect is essentially due to the introduction of a periodic disturbance of the main flow combined with the elevated levels of turbulence in the wakes. Therefore, the laminar – turbulent transition of the boundary layer flow on the suction side occurs earlier. This leads to increased losses at

high Reynolds numbers, where the flow on the suction side is fully attached, and decreased losses at low Reynolds numbers, where this effect reduces the size of the separation bubble.

Comparing the shape of the measured and the computed Re-lapse for steady conditions the loss generation seems reasonably captured by the CFD code. The computations are performed in 2D for a streamtube thickness adjustment for the divergent channel. The computation does not capture the significant loss decrease between $Re = 200k$ and $400k$, but actually it is not clear what causes this significant drop, since the separation bubble size is not very large any more at $Re = 200k$. At the lowest Re-number the suction side is fully separated (Although there is some pressure gradient recovery close to the trailing edge, Fig. 3.). The associated reduction in the Re-lapse seen in the experiment is not modelled by the computation. In older in-house cascades this lapse slope reduction has not been detected for Re-numbers of this range although it has been observed in literature. So far it is not clear whether this is a purely two-dimensional effect or whether the developing three-dimensionality of the cascade flow already has a strong effect.

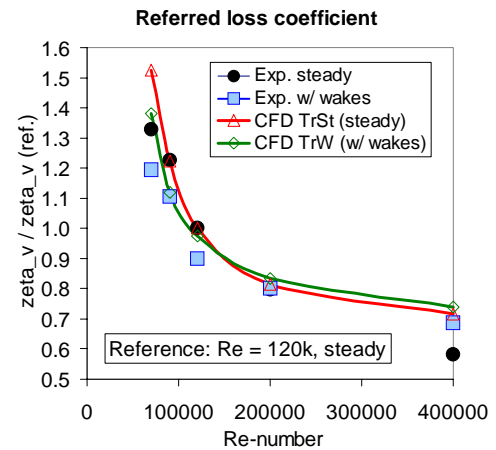


Figure 2: Referred loss coefficient as $f(Re)$ for T160 linear cascade

In the case of the incoming wakes the conventional CFD model is obviously not able to predict the reduced lapse rate. Just imposing the increased mean turbulence level due to the additional wake turbulence does not change the behaviour significantly. This is in line with experience from various turbine rig computations, where the Reynolds lapse rate is always overestimated using the conventional transition modelling, Gier et al. [16]. This gave the impulse to improve the simulation quality of transitional turbine boundary layer prediction through a transition model extension.

Basic Computational Procedure

Before the extension of the transition model is described, the employed CFD code is described briefly. The simulations are performed with the TRACE_S 3D compressible Navier-Stokes code, which is based on a block-structured finite volume scheme. The code computes the multiple rows fully coupled. Time integration to steady state is done using an implicit procedure. The convective fluxes are computed with a higher order MUSCL scheme combined with the flux differencing method of Roe. Convective fluxes are limited with a special version of the Van Albada Limiter. For the diffusive fluxes a

central scheme is employed. The stage coupling is based on the mixing plane technique with flux averaging and non-reflecting boundary interfaces and full mass conservation.

For turbulence modelling the Wilcox $k-\omega$ [17] two-equation model in low-Reynolds version was employed with extensions for compressibility and system rotation. The airfoil boundary layers are computed with low-Reynolds approach while in the rig computations wall functions are employed for the endwall regions. For more details, please refer to Gier et al. [18].

Transition Modeling

It is well known that the flow in low-pressure turbines is significantly governed by laminar-to-turbulent transition. Since “normal” two-equation turbulence models like the $k-\omega$ turbulence model, which is used in this code, are not able to reliably predict transition in a turbine environment, a transition model has to be employed. This is routinely done for a couple of years in the TRACE_S code used at MTU [18,19]. However, it is known that the predicted Re-lapse is too strong especially due to an overestimation of the separation bubble size at lower Re-numbers.

The transition model used is based on a model proposed by Drela [20], which is a reformulation of the correlations of Abu-Ghannam and Shaw [21]. Compared to the status of the model reported by Gier et al. [18] the basic model has been modified somewhat in recent years. It basically works by introducing an intermittency factor, which switches off turbulence production inside the boundary layer until a Reynolds-number parameter Re_{Θ_s} exceeds the momentum thickness Reynolds-number Re_{Θ} .

According to Drela [20], the Reynolds-number parameter Re_{Θ_s} is defined by:

$$Re_{\Theta_s} = 163 + 74.3 \left[0.55 \tanh \left(\frac{10}{H_{12} - 1} - 5.5 \right) + 1 \right] (0.94 n_{crit} + 1) \quad (1)$$

The parameter n_{crit} provides the influence of the free-stream turbulence taken at the boundary layer edge. Here a blend of 2 functions is used, since the correlation of Mack [22] is not appropriate for larger levels of free-stream turbulence, Arnal and Habiballah [23].

$$\begin{aligned} n_{crit} &= -8.43 - 2.4 \ln(Tu); Tu < 1.9\% (Mack) \\ n_{crit} &= -3.26 - 1.09 \ln(Tu); Tu > 1.9\% (Arnal) \end{aligned} \quad (2)$$

The momentum thickness Re-number is:

$$Re_{\Theta} = \frac{u_{\infty} \Theta}{\nu} \quad (3)$$

In combination with the $k-\omega$ model just using the intermittency as a digital switch is not appropriate. The reason is that in this case the $k-\omega$ model produces turbulence much too quickly leading to early transition and suppression of separation bubbles. In reality transition is a process, which takes some distance in flow direction and there are a couple of approaches to model the transition region like the algebraic model of Michelassi et al. [24] or the transport model of Steelant and Dick [25]. The first model had been used in earlier code versions, Gier et al. [18], but since the turbulence model also has some kind of hysteresis due to its transport equation formulation, this algebraic expression is actually not very appropriate. Therefore, a much simpler

intermittency function had been implemented, which in connection with the turbulence model gives a reasonable approximation of growth in turbulence intensity in the transition region. Like the function proposed by Michelassi et al. [24], fully turbulent conditions with $f_t = 1$ are reached, when $Re_{\Theta_s} \geq 2 \cdot Re_{\Theta}$.

$$f_t = \left(\frac{Re_{\Theta} - 1}{Re_{\Theta_s}} \right)^{\alpha} \quad 1 \leq \alpha \leq 2 \quad (4)$$

As mentioned above this transition model is based on experimental data of Abu-Ghannam and Shaw [21], who performed experiments in a steady-state wind tunnel. Hence, it cannot be expected that any effects of impinging wakes, which are always present in turbomachinery can be captured.

Therefore, an attempt was made to model the influence of the impinging wakes in the frame of steady computations using the above described transition model as a basis. The model was aimed to include the major influences and still be simple and numerically stable.

According to various publications on wake – boundary layer interaction, e.g., Mayle [14], Hodson [15] the increased free-stream turbulence connected with incoming wakes is a major parameter for earlier transition start. The second major effect is the kinematic interaction of the boundary layer with the passing wakes with effects like the negative jet and the calmed region e.g., Halstead et al. [26]. Both are simultaneously present.

In order to adjust the basic “steady” transition model described above to the influence of wakes, the first step was to address the influence of the increased turbulence. Actually, in a steady multistage computation the turbulence generated by the upstream airfoil rows is transported downstream, if an appropriate transport equation model like the $k-\omega$ model is used. Thus, the time-mean increase of turbulence is already captured. However, experience with the basic model showed, that even in the case of attached boundary layer flow at elevated Reynolds numbers this is not sufficient to assess the transition location moving upstream under unsteady conditions. Obviously, the periodically significant increase of free-stream turbulence inside the passing wakes, which can reach turbulence intensities of 10% or even more, Solomon [27], has a stronger impact on the transition than just an elevated steady state turbulence level.

Therefore, a modification was introduced, which amplifies the free-stream turbulence sensitivity of the model as a function of the wake reduced frequency f_{red} , which is the ratio of the time scale of the impinging wakes and convection time through the airfoil row.

$$f_{red} = \frac{f_{wakes} b_{ax}}{c_{ax}} = \frac{N_{airfoils,upstream_row} \cdot n_{rel} \cdot b_{ax}}{c_{ax}} \quad (5)$$

Some authors use true chord and exit velocity instead, but since the axial velocity is much more constant within the airfoil passage than overall velocity, this representation is more straightforward. The amplification of the sensitivity is done by multiplying the turbulence degree in the equation for n_{crit} (2) by a factor AF, figure 4:

$$AF = C_{AF1} f_{red}^2 + C_{AF2} f_{red} + 1; \text{ with } C_{AF1} = -0.95, C_{AF2} = 2.8 \quad (6)$$

At steady conditions the function AF recovers the original formulation and it is bounded above $f_{red} = 1.5$ at a value of 3 due to the

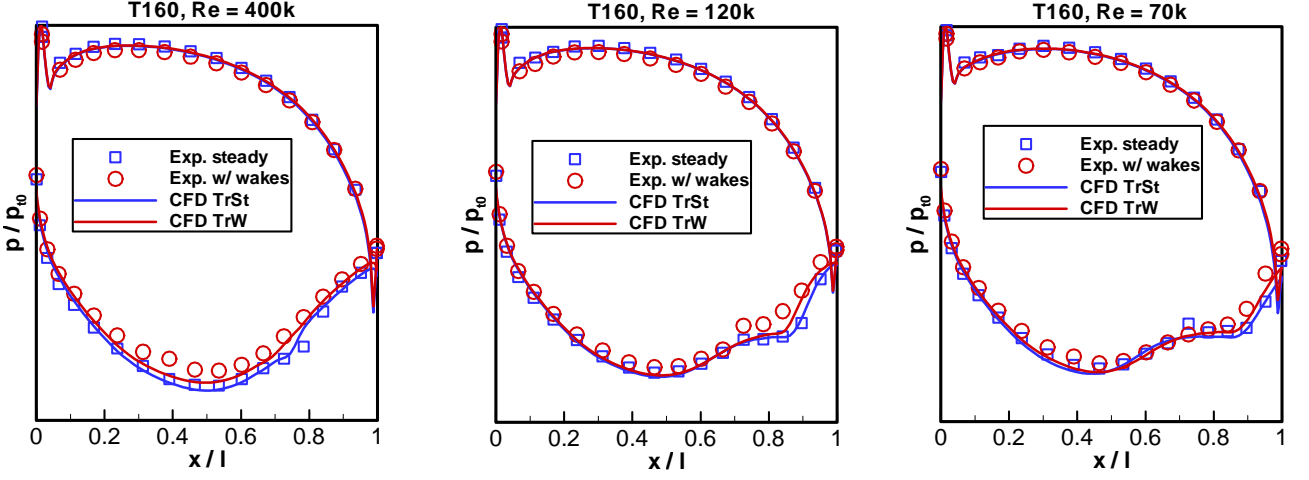


Figure 3: Profile pressure distributions vs. true chord, T160 for 3 Re-numbers

assumption that above $f_{red} = 1.5$ the wake passing effect is fully present, which has been reported e.g., by Coton et al. [28]. Actually, there are two influence factors one could include simultaneously, the reduced frequency and additional geometric relations like the ratio of the number of airfoils in two adjacent airfoil rows. However, there was not enough experimental data to calibrate a function with two variables and also these geometrical relations are usually not varying too much in LP turbines.

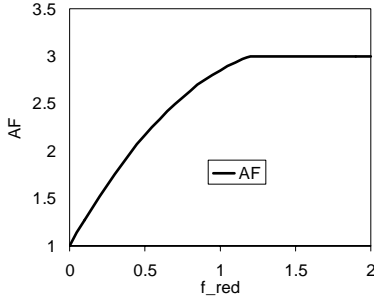


Figure 4: Amplification factor AF as function of reduced frequency

When employing this add-on for the T160 and other cascade tests it became obvious very quickly, that this amplification function works quite well in case of attached boundary layers. However, it is not able to predict the significant reduction of separation bubble size at lower Reynolds numbers.

In case of separation bubbles the wake passing must have an additional effect. Baniaghbal et al. [29] performed measurements in a linear cascade with aft loaded profiles and found that in case of separation bubbles the transition length was significantly more affected by the wakes than the transition location. This corresponds to in-house experience that only shortening the length of the transitional region enables the significant bubble size reduction under unsteady conditions.

The model expression developed regarding separation bubble size reduction assumes that under the influence of the passing wakes the transition length is reduced due to the kinematics of the wake – boundary layer interaction. This means that under fully attached flow

conditions the kinematic interaction is weak but in case of large bubbles its influence becomes strong. Hence the model expression has to take the reduced frequency and the bubble size into account.

Inside the basic model this influence can be introduced into the equation for the intermittency (4). In the basic formulation the intermittency is set to 1, if the ratio of Re_{Θ_s} and Re_{Θ} is two. Equation (4) is now modified in a way that by increasing the factor BF above 1 leads to a shortening of the transition length:

$$f_t = \min \left(1, \left(BF \cdot \left(\frac{Re_{\Theta}}{Re_{\Theta_s}} - 1 \right) \right)^{\alpha} \right) \quad (7)$$

The bubble influence factor BF is computed from equation (8):

$$BF = \min(2.5, f(f_{red}) \cdot f_b + 1) \quad (8)$$

The function introducing the influence of the reduced frequency is limited at a value of approximately 1.5 for reduced frequencies above 1.5, using the same frequency limit as for the expression for the turbulence influence.

$$f(f_{red}) = 1.5 \cdot \left(1 - e^{(-1.5 \cdot f_{red})} \right)^{\beta}; \text{ with } \beta = 0.4 \quad (9)$$

For the function representing the bubble size influence it is assumed according to experience that a very large separation bubble can be determined by the ratio of maximum reverse flow velocity u_{bubble} to free-stream velocity u_{∞} to reach 0.2. Hence, function (10) is designed to reach 1 at this value:

$$f_b = \left[\frac{\cos \left(\left(1 + \frac{u_{bubble}}{u_{\infty}} \cdot 5 \right) \cdot \pi \right)}{2} + \frac{1}{2} \right] \cdot \left[\left(C_B \left(0.2 - \frac{u_{bubble}}{u_{\infty}} \right) \cdot 5 \right)^{\gamma} + 1 \right] \quad (10)$$

with $C_B = 4.3, \gamma = 2.6$

This function starts with small values for small bubble sizes and then grows quickly. It has been calibrated with measurements in 3 different cascades (T106C, T106D [13], T160).

Results of this modelling are shown in figure 3, where the pressure distributions of the T160 cascade are plotted for three selected Reynolds numbers. For the highest tested Reynolds number 400,000 there is a very good agreement for both the steady conditions without incoming wakes and the case with incoming wakes. The presence of the wakes basically eliminated the separation bubble. In the cases of the two smaller Reynolds numbers the separation bubble is reduced by the wakes but it is still present. For steady conditions the computation again provides a very good prediction. In case of incoming wakes the bubble size is still slightly overpredicted by the CFD, but the main effect is captured.

As can be seen in figure 2, the model also predicts the loss Reynolds lapse rate pretty well. Except for the lowest Reynolds number, where the same applies as for the steady conditions, the trend is captured as well as the change compared to the steady conditions.

For all computations shown in this paper the transition model is only activated on the suction sides of the airfoils (on both sides of the non-turning strut in the turbine rig), because it is difficult to define a meaningful boundary layer edge on pressure sides. Under realistic conditions with typical free-stream turbulence levels the pressure side surface pressure distribution is hardly affected by the turbulence status in the boundary layer (The differences between measurements with and without wakes, figure 3, on the pressure sides is due to the difficult adjustment of inlet flow angle for the case with the wake generator.). The two-equation turbulence models often predict some turbulence production in the front part and some damping of turbulence in the strongly accelerating rear part of the pressure side. In case of strongly separated pressure side flows (not present in the airfoils in this paper) the current transition modelling approach is not appropriate anyway. Overall losses are not affected very significantly by this approach.

At this point it should be noted that this wake influence modelling uses a quite pragmatic approach. So far there is not very much reliable experimental data available for calibration of such a model. Also modelling such complex mechanisms like wake induced transition within a steady state simulation has to be used with some caution. However, the model is very stable and produces quite reasonable results. It only needs information, which is available from the basic model plus some integral information concerning turning speed and geometry. Like the basic model it needs boundary layer information, but apart from that it is a local formulation without the need to compute streamlines, pressure gradients, etc.

RIG TEST WITH 5-STAGE HSL TURBINE

Design of Test Turbine

To evaluate the concept of elevated stage loading for low pressure turbines a rig was designed and tested, which would be close enough to potential engine applications for larger commercial jet engines. Therefore, a 5-stage configuration was chosen with a design pressure ratio of approximately 4.8, which could still be tested in the Altitude Test Facility (ATF) at Stuttgart University. In the design point the test turbine has a stage loading factor $\Delta h/U^2$ of 2.6, which is about 20% higher than typical stage loading factors of low pressure turbines.

The flow path of the turbine rig is shown in figure 5. The rig has a

bladed inter-turbine duct, which realizes a relatively large shift in flow path radius in order to reach elevated circumferential velocity already in the front stages. The turbine itself has a relatively wide flow path. In the Smith chart this corresponds to a low through flow (LTF) design. This was chosen, because this results in low Mach number levels inside the turbine and improves the aspect ratio of the airfoils. In the T160 cascade, which has a turning of 107° , no major problems showed up concerning the stability of the suction side flow. Thus, a LTF-design with similar average turning seemed very reasonable.

The effect of increased turning is counteracted by the high aspect ratio of the airfoils. Furthermore, a LTF design results in better flow acceleration in the airfoil passages compared to higher through flow design options.

Except for the last stage the flow path grows steadily in diameter to improve the circumferential velocities. The slope of the outer diameter is significant but not at the absolute design experience limit. This was chosen to avoid excessive growth of secondary flows through the combination of outer endwall slope and high flow turning levels.

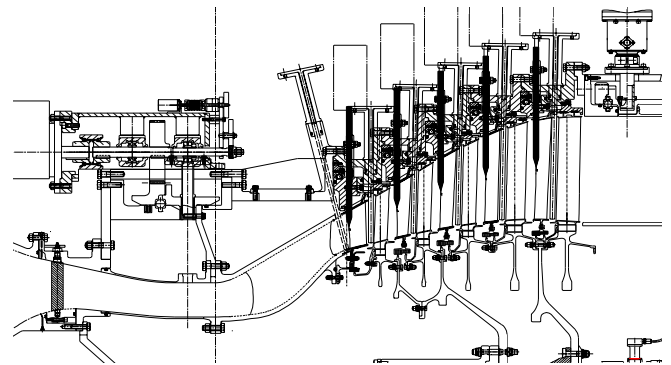


Figure 5: Rig arrangement

The turbine airfoils all have relatively high aspect ratios, especially the guide vanes of the last two stages, which have a cut-off design. Cut-off design was implemented, because most state-of-the-art low pressure turbines need this to achieve moderate noise levels. The high aspect ratio helps to control secondary flow impact, but it also leads to moderate Reynolds numbers. Especially the two rear stage vanes have a relatively low Reynolds number, which has to be considered during the airfoil design.

Due to the high turning levels of up to 110° average turning, thick airfoils have been designed, which would lead to hollow airfoils in a real engine. As also reported by Vázquez et al. [11] there is a significant efficiency loss associated with thin solid airfoils at these high turnings due to large pressure side separation bubbles. As also seen e.g., in figure 11 the profile pressure distribution features aft loading in combination with controlled loading of the front.

The test turbine has been heavily instrumented to measure radial distributions of pressure and temperature at turbine inlet and outlet as well as between the stages. Also pressure taps have been instrumented on three radial locations on all vane rows. A view of the instrumented turbine installed in the test facility in Stuttgart is shown in figure 6. The test program included 4 speed lines and a Reynolds lapse rate with 4 Reynolds numbers

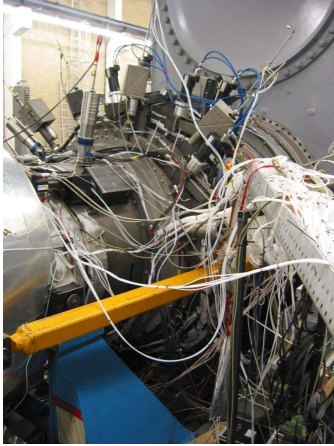


Figure 6: Test turbine installation in ATF Stuttgart

Results and Analysis

In figure 7 the achieved efficiencies are plotted versus pressure ratio for the 4 speed lines. The typical behaviour for turbines with a number of stages can be seen. The efficiency sensitivity with respect to pressure ratio is quite low for the higher turning speeds. Only at 80% design speed the sensitivity is somewhat stronger. For the higher turning speeds and pressure ratios the sensitivity is small, because for a given turning speed basically only the rear stage is running at higher stage pressure ratio. And since in this turbine even the rear stages are still subsonic the slight increase in loss for the last stage is more or less compensated by the change in stage work split (The more efficient rear stage takes more work from the front stages.)

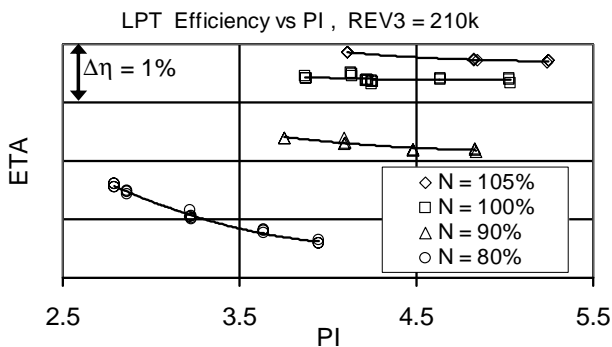


Figure 7: Turbine efficiency map for cruise Reynolds number

Another interesting characteristic for this high stage loading turbine is the Reynolds lapse rate. Going to higher stage loading leads to the combination of reduced flow acceleration and increased turning, which puts more load onto the suction side flow. Without increasing the number of airfoils or axial chord, which is undesirable for cost and weight reasons, this results in higher airfoil loading. Hence, it can be expected that especially at lower Reynolds numbers it becomes increasingly difficult to avoid flow separation and significant loss increase. Therefore, this rig has some additional instrumentation, which was intended to support analysis of lower Reynolds number conditions.

In figure 8 the turbine efficiency is displayed for 100% speed and design pressure ratio with the efficiency value at $Re = 210k$ taken as reference for each curve. The numbers are referred to the cruise condition of 1st vane Reynolds number of 210k, which is equivalent to 35000 ft altitude. It can be seen that for the 3 Reynolds numbers between 170k and 270k the lapse rate is only slightly changing. Hence, the flow structure can be expected to remain fairly unchanged with only moderate growth of reattached separation bubbles. Only at the lowest investigated Reynolds number the slope starts to increase, indicating accelerated growth of separation bubbles.

In figure 8 also the results of the current CFD predictions are included with the basic steady transition model (TrSt) and the above described wake transition model (TrW). While the steady model significantly overpredicts the Reynolds lapse rate even for the higher Reynolds numbers, the wake transition model improves the simulation quite a bit. Between the two higher Reynolds numbers the new model predicts the lapse almost exactly. For lower Reynolds numbers it still overpredicts the lapse to some small extent, which is in line with the results from the T160 cascade. Hence, the new model still tends to overestimate the size of the separation bubbles. Although this is not perfect from a computation and analysis point of view it gives the designer some confidence that in reality a certain design will have a safely reattached boundary layer.

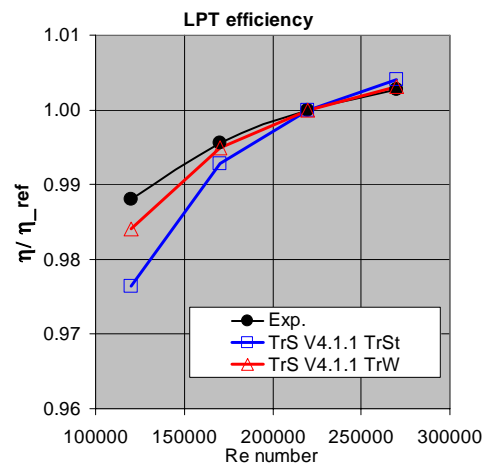


Figure 8: Turbine efficiency lapse rate comparison, $n = 100\%$

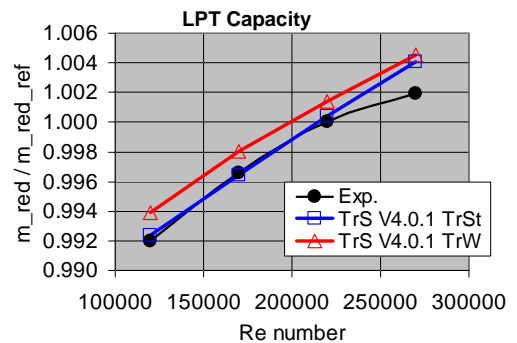


Figure 9: Reduced turbine massflow as function of Reynolds number

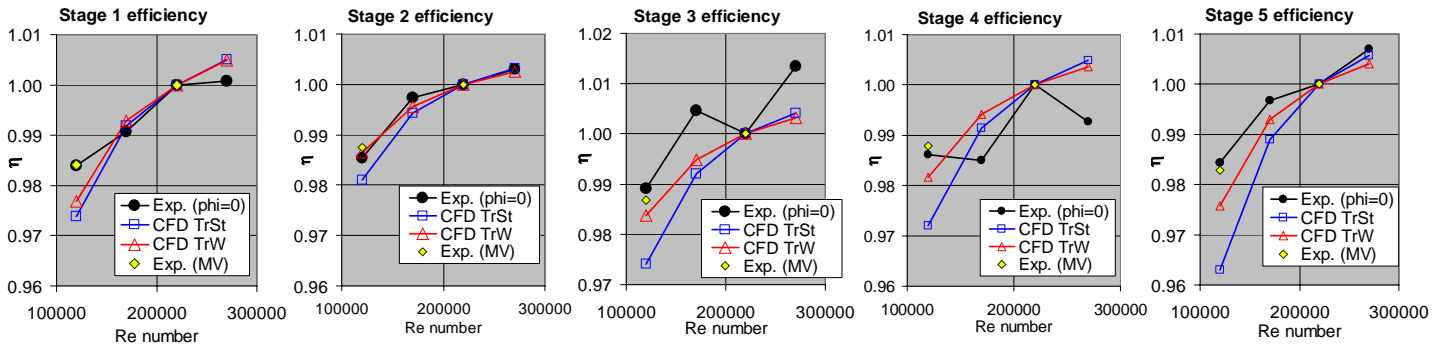


Figure 10: Referred stage efficiencies in all 5 stages of test turbine, comparison of measured and computed data

As can be seen in figure 9 the turbine capacity is relatively constant with Reynolds number variation. The prediction, which is based on throat area corrected airfoils, captures level and sensitivity very accurately. The small difference ($<0.2\%$) between the 2 computations is probably due to the difference in turbine efficiency as higher losses lead to smaller capacities. The difference to the measurement is well within the accuracy of the hardware quality.

Because evaluating integral efficiencies of a 5-stage turbine averages out a lot of details, inter-stage instrumentation has been added to the test rig. The resulting efficiency lapse is shown in figure 10 for all 5 stages. For the experiment two sets of data are displayed. The black points are taken at a certain circumferential position, while the yellow-black diamonds correspond to a circumferential traverse, which is more accurate. Unfortunately this traverse was only done for two Reynolds numbers due to time constraints.

Keeping in mind that inter-stage measurement involves more data scatter and probe - blade row interaction, the agreement between measurement and computation is very reasonable. The efficiency lapse of the middle 3 stages is very similar at about 1.2 % between Reynolds numbers of 210k and 120k indicating no separation problem in these stages in this Reynolds range. The lapse of the first stage is actually

slightly higher. Although there could be also an issue concerning influence of incoming endwall boundary layer (which also changes with Reynolds number in the entire test rig configuration) the computation indicates that there might be an effect in the blading. Actually the CFD computes an overproportional loss increase in the first rotor blade, although the separation bubble still reattaches upstream of the trailing edge.

In the last stage, where at this operating point the cut-off vane operates at Reynolds numbers of below 70,000 the Reynolds lapse is significantly increased. The CFD computation shows the same characteristics as for the overall efficiency and the T160 cascade. While it is very close to the experiment in the 2nd stage, the differences become larger for the rear stages, which have the lower Reynolds numbers. However, the wake transition model produced a significant improvement for the CFD prediction.

To take a closer look into the flow the surface pressure distributions of the 3rd vane are shown in figure 11 for the 3 radial locations at design conditions. In all pressure diagrams experimental data, steady and wake transition model CFD computations are displayed. At design conditions ($Re = 210k$ at 1st vane as reference operating point Reynolds number) the 3rd vane operates at a Reynolds

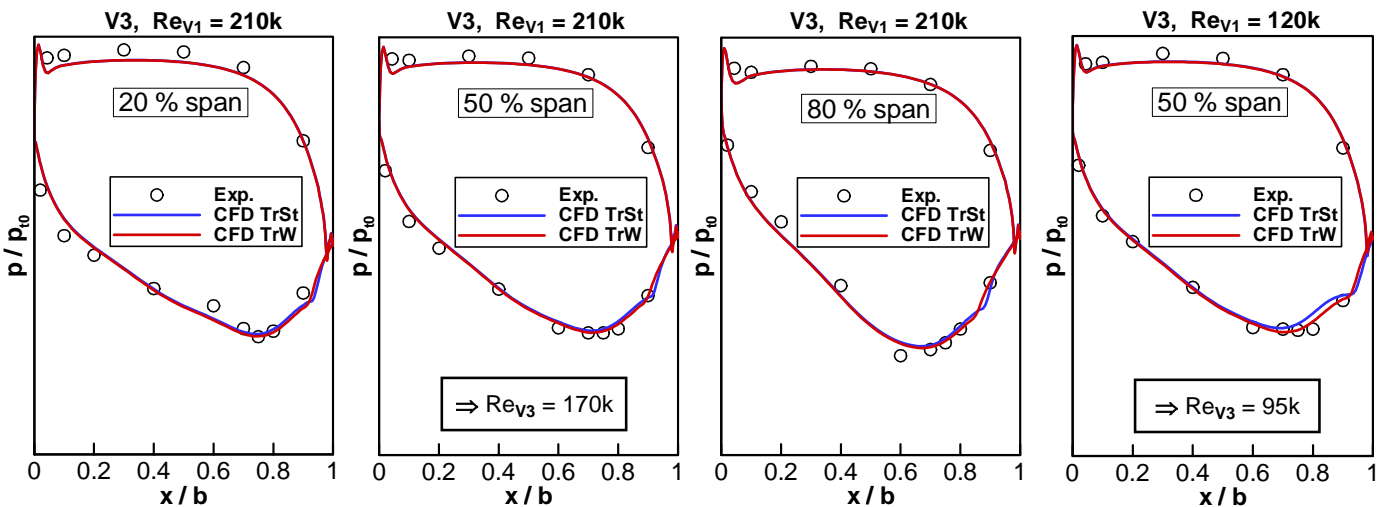


Figure 11: Surface pressure distributions on 3 radial locations on 3rd vane for design Reynolds number and midspan for low Reynolds number

number of 170,000. As mentioned above the pressure distribution is a rear loaded design with sufficient acceleration and controlled level of diffusion. The airfoil has 111° turning on average and a Zweifel number load parameter close to one.

On the suction side there is a small separation bubble, which can be seen in the starting formation of a plateau of the suction side pressure distribution at around 90 % axial chord. The CFD code results correspond quite nicely with the measured data for all 3 radial locations. The two transition models hardly differ for the design Reynolds number (Re 210k), but at 50 % span the wake transition model seems to provide an even slightly better agreement with measurement. In the right picture of figure 11 the midspan distribution is plotted for the low Reynolds number case. Although the density of the measured data is not very fine, the wake model again seems to compute a better agreement with data.

In figure 12 the midspan pressure distribution of vane 4 is shown. This slice has been instrumented much more densely in the bubble region of the suction side. Again, both computations produce a reasonable agreement with the data, but the wake model seems to predict the small bubble size better. At the lower Reynolds number, which corresponds to a vane 4 Reynolds number of 75,000, the steady transition model simulation clearly overpredicts the size of the separation bubble, leading to the too large Reynolds lapse rate as discussed above. Even the wake transition model (TrW) seems to overpredict the bubble size.

The pressure distribution in figure 12 indicates that at least at midspan a reattached flow can be expected on the suction side. However, since even a boundary layer, which shows a pressure distribution plateau with recovering pressure gradient, might still not be reattached, surface streamlines are plotted in figure 13. Here, the suction side of vane 4 can be seen for all 4 Reynolds numbers. It is obvious that the separation bubble size grows with decreasing Reynolds number. At Re = 120k, the reattachment close to the hub becomes borderline.

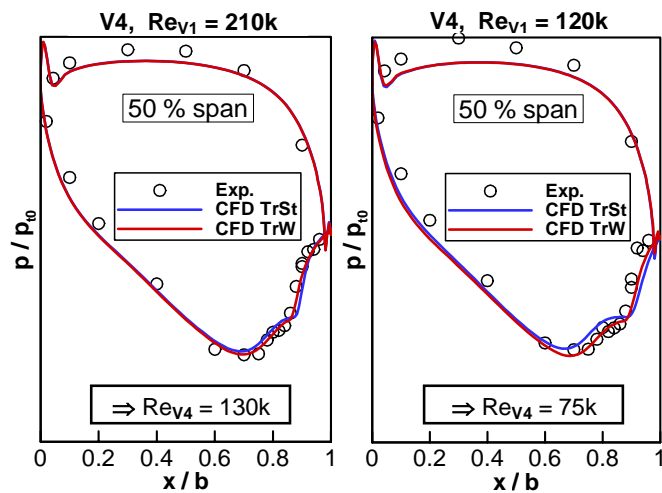


Figure 12: Surface pressure distributions on 4th vane for 2 Reynolds numbers

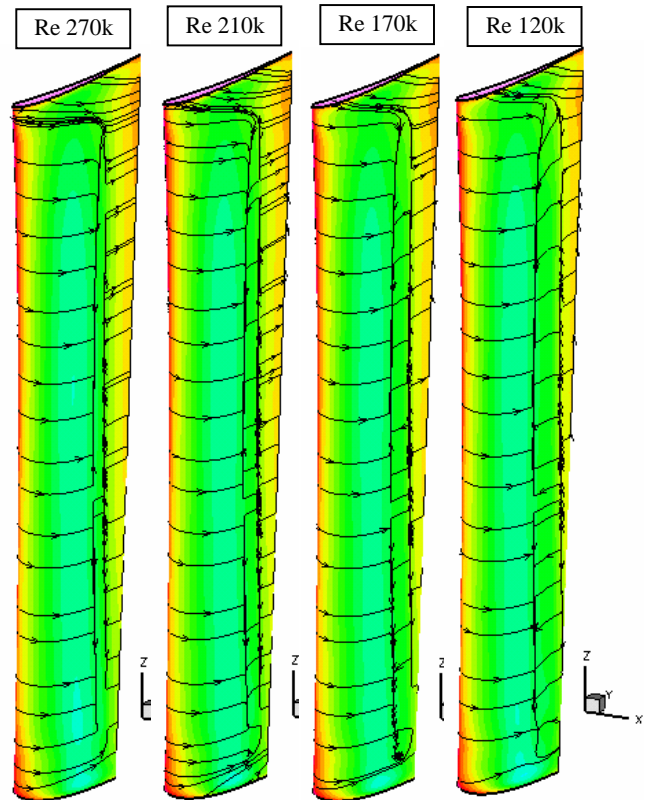


Figure 13: Surface streamlines and static pressure on vane 4 airfoil (computations with wake transition model)

Taking a closer look into the surface streamlines in figure 13 reveals that the separation bubble growth with decreasing Reynolds number is quite steady except for the lowest Reynolds number. In figure 14 the computed separation bubble length measured at midspan is shown for this airfoil. Between Reynolds numbers of 170,000 to 270,000 there is almost a linear variation with Reynolds number. However, at the lowest Reynolds number the bubble growth accelerates. This corresponds exactly with the efficiency development with Reynolds number for stage 4 seen in figure 10.

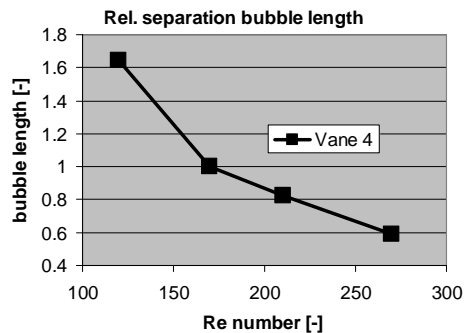


Figure 14: Separation bubble length at midspan of vane 4 based on CFD prediction

Finally taking a look into the radial efficiency distribution (Fig. 15) it can be seen that the efficiency at midspan is reproduced very

well by the computation (TrW). The overprediction close to the endwalls is typical for computations of the ideal flow path as discussed by Gier et al. [16]. Without computing or modelling the real endwall geometry and leakages the losses in the proximity of the endwalls are underpredicted.

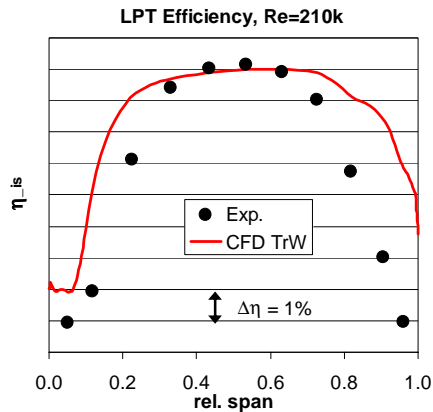


Figure 15: Distribution of turbine efficiency at design conditions

CONCLUSIONS

In this paper the design and analysis of a 5-stage low pressure turbine rig with high stage loading is described. The measured performance characteristics corresponded well with pre-test expectations and demonstrate that turbines at this stage loading level can still have high levels of efficiency far above $\eta_{is} = 90\%$. Through the chosen design philosophy the turbine also behaved very smoothly within the operating map.

The design was supported by definition and testing of a linear cascade airfoil with elevated turning compared to past experience. This airfoil was tested with a wake generator, resulting in a significantly reduced Reynolds lapse rate. Since the available transition model was not able to predict this behavior, a modification had to be developed.

This modified transition model takes the influence of the wakes onto the time mean flow into account. It is based on simplifications of the basic influence mechanisms on wake induced transition. The additional correlations were calibrated for a couple of impinging wake cascade tests.

The enhanced model significantly improves prediction quality especially for suction side flow in the presence of separation bubbles. The predicted lapse rates for the cascade test as well as for the 5-stage rig came out considerably better than with the basic model. Similar trends can be recognized also for other low pressure turbine rigs.

In a more detailed look into the main flow physics of the high stage loading turbine rig it became clear that the current design still has a good performance potential at least for a 20% reduced Reynolds number. Only below this level, the cut-off vanes of the last 2 stages start to separate leading to increased loss production.

Future work in this area will focus on further improving simulation quality. Also it could be worthwhile looking into combining high stage loading and high airfoil loading and possibilities to maintain the desired efficiencies.

ACKNOWLEDGEMENT

The authors wish to thank MTU Aero Engines for permission to publish this paper.

REFERENCES

- [1] Smith, S.F., 1965, "A Simple Correlation of Turbine Efficiency", *J. of Royal Aeronautical Society*, Vol. 69, July
- [2] Traupel, W., 1966, "Thermische Strömungsmaschinen", Springer Verlag
- [3] Denton, J.D., 1993, "Loss Mechanisms in Turbomachines", *ASME paper 93-GT-435*
- [4] Gregory-Smith, D.G., Graves, C.P., Walsh, J.A., 1988, "Growth of Secondary Losses and Vorticity in a Turbine Cascade", *J. of Turbomachinery*, Vol. 110, No. 1, p. 1
- [5] Whitney, W.J., Behning, F.P., Moffitt, T.P., Hotz, G.M., 1977, "Cold-Air Investigation of 4 1/2 - Stage Turbine with Stage Loading Factor of 4.66 and High Specific Work Output", NASA Technical Memorandum, TM X-3498
- [6] Moustapha, S.H., Okapuu, U., Williamson, R.G., 1987, "Influence of Rotor Blade Aerodynamic Loading on the Performance of a Highly Loaded Turbine Stage", *J. of Turbomachinery*, Vol. 109, pp. 155 – 162
- [7] Schaub, U.W., Vlastic, E., Moustapha, S.H., 1993, "Effect of Tip Clearance on the Performance of a Highly Loaded Turbine Stage", AGARD Meeting on 'Technology Requirements for Small Gas Turbines'
- [8] Vlastic, E.P., Girgis, S., Moustapha, S.H., 1995, "The Design and Performance of a High Work Research Turbine", *ASME Paper 95-GT-233*
- [9] Kawachi, Y., Shimizu, K., Nogami, R., 2000, "Research and Development of Highly-Loaded Turbine", *AIAA Paper 2000-3639*
- [10] Haller, B., Anderson, J., 2002, "Development of New High Load/High Lift transonic Shrouded HP Gas Turbine Stage Design – A New Approach for Turbomachinery", *ASME Paper GT-2002-30363*
- [11] Vázquez, R., Cadrecha, D., Torre, D., Morales, M., 2001, "Low Pressure Turbine with High Stage Loading", *ISABE Paper 2001-1060*
- [12] Vázquez, R., Cadrecha, D., Torre, D., 2003, "High Stage Loading Low Pressure Turbines. A New Proposal for an Efficiency Chart", *ASME Paper GT2003-38374*
- [13] Stadtmüller, P., Fottner, L., Fiala, A., 2000, "Experimental and Numerical Investigation of Wake-Induced transition on a Highly Loaded Turbine at Low Reynolds Numbers", *ASME Paper 2000-GT-0269*
- [14] Mayle, R.E., 1991, "The Role of Laminar – Turbulent Transition in Gas Turbine Engines", *J. of Turbomachinery*, Vol. 113, pp. 509 – 537
- [15] Hodson, H.P., 1990, "Modeling Unsteady Transition and its Effects on Profile Loss", *J. of Turbomachinery*, Vol. 112, No. 3
- [16] Gier, J., Stubert, B., Brouillet, B., de Vito, L., 2003, "Interaction of Shroud Leakage Flow and Main Flow in a Three-Stage LP Turbine", *ASME paper GT2003-38025*
- [17] Wilcox, D.C., 1988, "Reassessment of the Scale Determining Equation for Advanced Turbulence Models", *AIAA Journal*, Vol. 25, No. 11, pp. 1299 – 1310

- [18] Gier, J., Ardey, S., Heisler, A., 2000, "Analysis of Complex Three-Dimensional Flow in a Three-Stage LP Turbine by means of Transitional Navier-Stokes Simulation", ASME Paper 2000-GT-645
- [19] Gier, J., Ardey, S., 2001, "On the Impact of Blade Count Reduction on Aerodynamic Performance and Loss Generation in a Three-Stage LP Turbine", ASME Paper 2001-GT-197
- [20] Drela, M., 1995, "Implementation of Modified Abu-Ghannam/Shaw Transition Criterion", MIT Aero-Astro
- [21] Abu-Ghannam, B.J., Shaw, R., 1980, "Natural Transition of Boundary Layers – The Effects of Turbulence, Pressure Gradient and Flow History, *J. of Mechanical Engineering Science*, Vol. 22, No. 5, pp. 213 – 228
- [22] Mack, L.M., 1977, "Transition and Laminar Instability", Jet Propulsion Laboratory Publication 77-15, Pasadena, CA
- [23] Arnal, D., Habiballah, M., 1979, "Resolution Numerique des Equations de Stabilité de la Couche Limite Laminaire. Comparaison aux Resultats Experimentaux Obtenus au Derat", rapport Technique OA n° 10/5018
- [24] Michelassi, V., Rodi, W., Gieß, P.A., 1998, "Experimental and Numerical Investigation of Boundary-Layer and Wake Development in a Transonic Turbine Cascade", *Aerospace Science and Technology*, No. 3, 191 – 204
- [25] Steelant, J., Dick, E., 2001, "Modeling of Laminar-Turbulent Transition for High Freestream Turbulence", *J. of Fluids Engineering*, Vol. 123, No. 1
- [26] Halstead, D.E., Wisler, D.C., Okiishi, T.H., Walker, G.J., Hodson, H.P., Shin, H., 1997, "Boundary Layer Development in Axial Compressors and Turbines: Part 1- Composite Picture; Part 3 – LP Turbines; Part 4- Computations and Analyses", *J. of Turbomachinery*, Vol. 119, pp. 114 – 127, 225 – 237, 128 – 139
- [27] Solomon, W.J., 2000, "Effects of Turbulence and Solidity on the Boundary Layer Development in a Low pressure Turbine", ASME paper 2000-GT-0273
- [28] Coton, T., Arts, T., Lefebvre, M., Liamis, N., 2002, "Unsteady and Calming Effects Investigation on a Very High lift LP Turbine Blade – part I: Experimental Analysis", ASME Paper GT-2002-30227
- [29] Baniaghbal, M.R., Curtis, E.M., Denton, J.D., Hodson, H.P., Huntsman, I., Schulte, V., 1995, "Wake passing in LP Turbine Blades", pres. At AGARD PEP 85th Symposium on 'Loss Mechanisms and Unsteady Flows in Turbomachines', Derby, UK